Quaternary Science Reviews 242 (2020) 106443

Contents lists available at ScienceDirect

Quaternary Science Reviews

journal homepage: www.elsevier.com/locate/quascirev

Stability of the Atlantic overturning circulation under intermediate (MIS3) and full glacial (LGM) conditions and its relationship with Dansgaard-Oeschger climate variability

Xiao Zhang [a, *], Matthias Prange [b]

[a] Nanjing University of Information Science and Technology, China
[b] MARUM – Center for Marine Environmental Sciences, University of Bremen, Germany

ARTICLE INFO

Article history:
Received 19 February 2020
Received in revised form
11 June 2020
Accepted 18 June 2020
Available online xxx

Keywords:
Last glacial maximum
Marine isotope stage 3
Paleoclimate modeling
Abrupt climate change
Dansgaard-Oeschger events
Atlantic meridional overturning circulation

ABSTRACT

Paleoclimatic records reveal that millennial-scale climate variability during the Pleistocene was most pronounced during intermediate glacial conditions, like Marine Isotope Stage 3 (MIS3), rather than during interglacial and fully glaciated climates, like the Last Glacial Maximum (LGM). The rapid transitions between cold stadials and warm interstadials recorded in Greenland ice cores during MIS3, referred to as Dansgaard–Oeschger (D-O) events, have been correlated with millennial-scale climate variations worldwide. Although the origin of D-O events is a matter of controversy, striking evidence shows that variations in the strength of the Atlantic meridional overturning circulation (AMOC) were involved. Therefore, understanding the stability properties of the ocean circulation under different background climate conditions is key to understanding D-O millennial-scale climate variability. In the present study, the stability of the AMOC to northern high-latitude freshwater perturbations under MIS3 and LGM boundary conditions is investigated by using the coupled climate model CCSM3. Stability diagrams constructed from a large set of equilibrium experiments reveal a nonlinear dependence of AMOC strength on freshwater forcing under both MIS3 and LGM conditions. The MIS3 baseline state is close to an AMOC stability threshold, which makes the MIS3 climate unstable with respect to minor perturbations. A similar threshold behavior in AMOC stability is observed under LGM conditions; however, larger freshwater perturbations are necessary to pass the threshold and weaken the AMOC. The threshold's displacement relative to the MIS3 background climate is attributable to differences in the atmospheric hydrologic cycle and North Atlantic sea ice transport. Different atmospheric moisture transports are attributable to thermodynamic and dynamic processes related to differences in greenhouse gas forcing and ice-sheet height between MIS3 and the LGM. We conclude that the higher stability of the AMOC during the LGM is a physically plausible explanation for millennial-scale D-O-type climate variability being suppressed under full glacial conditions, whereas minor perturbations in freshwater fluxes could have triggered D-O climate shifts during MIS3.

1. Introduction

Millennial-scale variability with a bipolar seesaw pattern is a typical feature of Pleistocene climates and has been documented in paleoclimatic records worldwide (e.g. Voelker, 2002). A recent investigation of the long-term characteristics of climate variability based on an Antarctic ice core record has shown that millennial-scale variability has been most pronounced under intermediate glacial climate conditions, as compared to more stable interglacial and full glacial conditions (Kawamura et al., 2017). During the last glacial cycle, this characteristic has been evident in the frequent and pronounced occurrence of Dansgaard-Oeschger (D-O) events during the intermediate glacial climate of Marine Isotope Stage 3 (MIS3; approx. 25–60 ka ago), whereas D-O events were absent during the full glacial conditions (i.e. minimum global sea level and greenhouse gas concentrations) of the Last Glacial Maximum (LGM) and the interglacial conditions of the Holocene (Fig. 1; Grootes and Stuiver, 1997; Schulz et al., 1999). Proxy records (Fig. 1; Sarnthein et al., 2001; Henry et al., 2016) and model studies (e.g.

* Corresponding author.
E-mail address: xzhang@nuist.edu.cn (X. Zhang).

https://doi.org/10.1016/j.quascirev.2020.106443
0277-3791/

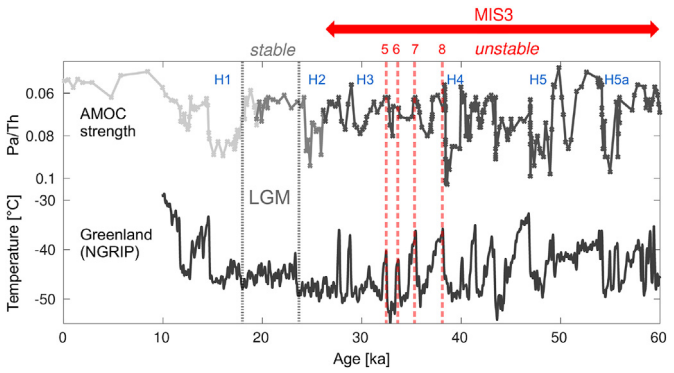

Fig. 1. Reconstruction of AMOC strength, based on Pa-231/Th-230 ratios from Bermuda Rise sediment cores (light gray: McManus et al., 2004; gray: Lippold et al., 2009; dark gray: Henry et al., 2016) and Greenland (NGRIP) temperature (Kindler et al., 2014) for the past 60,000 years. The stable climate of the LGM is highlighted. D-O interstadials 5–8 exemplify the unstable climate of MIS3, whereas Heinrich stadials (H1–H5a) also occur outside MIS3.

Ganopolski and Rahmstorf, 2001) suggest that D-O-type climate variability with a bipolar seesaw pattern (EPICA Community Members, 2006; WAIS Divide Project Members, 2015) is tied to variations in the Atlantic meridional overturning circulation (AMOC) and its associated heat transport. Combining climate model results with sea surface temperature (SST) proxy records covering MIS3, Zhang et al. (2015) estimated a reduction in the AMOC's strength of about 9 Sv (1 Sv = 10^6 m^3/s) during (non-Heinrich) stadial states (i.e. millennial-scale colder phases in northern latitudes), as compared to interstadial states (i.e. millennial-scale warmer phases). Given the close link between millennial-scale climate variability and the AMOC, it is natural to hypothesize that the occurrence or absence of D-O-type variability during specific stages is attributable to the changing stability properties of the ocean circulation, which may depend on climatic boundary conditions such as ice-sheet volumes and greenhouse gas concentrations (e.g. Prange et al., 1997; Ganopolski and Rahmstorf, 2001; Prange et al., 2002; Romanova et al., 2004). More specifically, D-O events being infrequent or absent during full glacial stages may point to high stability of the AMOC, whereas the pronounced D-O variability during MIS3 may be indicative of a more vulnerable ocean circulation.

In a previous study, we investigated the stability properties of the AMOC using the coupled atmosphere-ocean general circulation model (AOGCM) CCSM3 under MIS3 boundary conditions (Zhang et al., 2014b). We found a highly nonlinear dependence of the AMOC's strength on freshwater forcing at high northern latitudes and a remarkably unstable MIS3 baseline state, such that small perturbations in the order of 0.02 Sv could trigger stadial-interstadial climate anomalies. We therefore concluded that minor perturbations in the hydrologic cycle, e.g. related to ice sheet processes and meltwater fluxes (van Kreveld et al., 2000; Elliot et al., 2002), could trigger D-O-type climate shifts.

The present study complements our previous work by investigating the stability of the AMOC under full glacial (LGM) conditions and comparing the LGM's stability properties with those of MIS3. Our results suggest an AMOC that was more stable under full glacial than under intermediate glacial conditions and hence provide a physically plausible explanation for the absence (occurrence) of D-O variability during the LGM (MIS3).

2. Model and experimental design

2.1. Model description

Climate model experiments were performed with the National Center for Atmospheric Research's (NCAR's) Community Climate System Model version 3 (CCSM3), which is a fully coupled AOGCM consisting of four model components that represent the atmosphere, land, ocean, and sea ice (Collins et al., 2006; Yeager et al., 2006). The atmosphere and land components share the same T31 horizontal resolution (3.75° transform grid) with 26 layers (hybrid coordinates) in the atmosphere. The land model was improved with new parameterizations for canopy interception and soil evaporation (Oleson et al., 2008), and a dynamic global vegetation model was activated in our simulations (Mohtadi et al., 2014). The ocean component has a nominal horizontal resolution of 3° with latitudinal refinement about the equator (100 × 116 grid points) and 25 vertical levels. The North Pole is displaced over Greenland to avoid time-step constraints. The sea ice component uses the same horizontal grid as the ocean.

2.2. LGM (21 ka) baseline simulation and freshwater perturbation experiments

The LGM experimental setup follows the Paleoclimate Modelling Intercomparison Project 2 (Braconnot et al., 2007). The atmospheric greenhouse gas concentrations were set as follows: CO_2 185 ppmv, CH_4 350 ppbv, and N_2O 200 ppbv. The orbital parameters were applied for 21 ka, and a sea level lowering of 120 m was assumed, leading to changes in the land/sea distribution compared to present day, e.g. the closing of the Bering Strait. The implemented ice sheet configuration for 21 ka was based on the ICE-5G model (Peltier, 2004). Ozone and aerosol distributions were kept at pre-industrial levels (Otto-Bliesner et al., 2006).

The basic LGM experiment was integrated for 2000 years, and at model year 1500, three hosing experiments were branched off with different rates of continuous, unbalanced surface freshwater flux (applied as virtual salinity fluxes, e.g. Prange and Gerdes, 2006) homogeneously distributed over the Nordic Seas. Each hosing experiment was integrated for 500 years with freshwater input rates of 0.02 Sv, 0.05 Sv, and 0.2 Sv.

2.3. MIS3 (38 ka) baseline simulation and freshwater perturbation experiments

The MIS3 baseline experiment was branched off from model year 1500 of the LGM run and integrated for another 2170 years. Boundary conditions for 38 ka were applied, including orbital parameters and the ICE-5G ice sheet configuration, with a corresponding sea level reduction (Peltier, 2004). The following greenhouse gas concentrations were taken from ice core data (Flückiger et al., 2004; Spahni et al., 2005; Ahn and Brook, 2007; Bereiter et al., 2012): CO_2 215 ppmv, CH_4 501 ppbv, and N_2O 234 ppbv. The 38 ka time slice was chosen because it lies right in the middle of a rather regular sequence of D-O cycles.

At model year 3170, 12 freshwater hosing/extraction experiments, as described above for the LGM, were branched off (with the amount of freshwater ranging from ±0.005 Sv to ± 0.2 Sv). Zhang et al. (2014b) showed that the integration time for all of these freshwater perturbation experiments was long enough for the AMOC to reach a new equilibrium. For more details on these simulations, see Zhang et al. (2014b). All mean climate states presented in this study are based on the last 100 years of each experiment.

3. Results

The basic states of both the LGM and MIS3 are characterized by vigorous AMOCs, with similar maximum North Atlantic overturning at around 15 Sv, which is about 1 Sv stronger than in the pre-industrial control run of the same model (cf. Zhang et al., 2014b). However, the southward flow of North Atlantic deep water is several hundred meters shallower in both glacial climate states than in the pre-industrial control run (not shown). Both the LGM and the MIS3 AMOC show a distinctly nonlinear response to freshwater forcing, as seen in the AMOC stability diagram (Fig. 2). For MIS3, this has been extensively discussed in Zhang et al. (2014b). In summary, the MIS3 AMOC's equilibrium response to freshwater hosing is characterized by an abrupt drop in overturning strength, for a forcing between 0.01 Sv and 0.02 Sv, associated with a southward displacement of the sea ice margin from the Nordic Seas to the North Atlantic as well as convective instability in the Nordic Seas. It has been shown (Zhang et al. 2014b, 2015) that climate states to the left of the threshold (i.e. with stronger AMOC) correspond to interstadials, whereas climate states to the right of the threshold (i.e. with weaker AMOC) correspond to stadials. In particular, the simulated interstadial-stadial difference in central Greenland surface temperature of 8–11 °C is in line with ice-core reconstructions (Fig. 1; Huber et al., 2006; Landais et al., 2004; Kindler et al., 2014). Moreover, recovery of the AMOC after removal of the freshwater hosing suggests that the MIS3 baseline AMOC was mono-stable (Zhang et al., 2014b).

For the LGM experiments, the AMOC stability diagram shows similar behavior as that under MIS3 conditions. Although much fewer hosing experiments have been performed under LGM conditions (due to limited computer resources), a distinct threshold can be identified in the stability diagram. This AMOC threshold is located between 0.02 and 0.05 Sv, i.e. to the right of the AMOC threshold of MIS3. This implies that the AMOC is more stable with respect to freshwater perturbations under LGM conditions than under MIS3 conditions, i.e. a stronger forcing is required to induce substantial weakening of the AMOC under full glacial conditions than under intermediate glacial conditions.

In both cases, the AMOC stability threshold is related to a collapse of convection and hence deep water formation in the Nordic Seas. Both basic states are characterized by active convection in the Nordic Seas just south of the winter sea ice margin (Fig. 3a and b). Compared to the MIS3 basic state, the maximum convection is shifted slightly southeastward in the LGM state. In response to a small freshwater hosing into the Nordic Seas, convection was slightly weakened in both cases (Fig. 3c and d). Just left of the AMOC threshold (i.e. for a 0.01 Sv hosing in the MIS3 case and a 0.02 Sv hosing in the LGM case), the winter sea ice margin slightly advanced, and the region of convection shifted to the east in the LGM case (Fig. 3d), whereas the region of convection stayed in place (at ca. 10° E) in the MIS3 case. A further increase in freshwater forcing leads to a collapse of convection and complete sea ice coverage in the Nordic Seas in both cases (Fig. 3e and f). The immobility and resulting vulnerability of the Nordic Seas' convection in the MIS3 case can be understood as resulting from a strong density stratification in the southern Norwegian Sea. To first order, density stratification is determined by salinity in the polar and subpolar seas. Fig. 4 shows the difference in salinity stratification between the basic states of MIS3 and LGM. In the southern Norwegian Sea, a stronger stratification was found in the MIS3 state compared to the LGM state, which prevented a shift of convection into this area in the MIS3 case. We identified three mechanisms that explain surface freshening and hence the stronger salinity stratification in the southern Norwegian Sea under MIS3 conditions, ultimately causing convection to be more vulnerable during MIS3 compared to LGM.

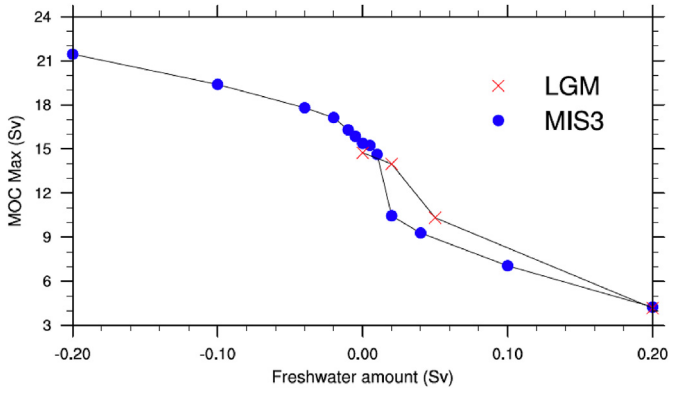

Fig. 2. AMOC stability diagram for the MIS3 (blue dots) and LGM (red crosses) boundary conditions. The AMOC (Sv) is shown as a function of freshwater perturbation (Sv) for equilibrium climate states. AMOC strength is defined as the maximum value of the overturning stream function below 300 m depth in the North Atlantic. Positive perturbations correspond to freshwater input to the Nordic Seas, while negative perturbations correspond to freshwater removal. (For interpretation of the references to colour in this figure legend, the reader is referred to the Web version of this article.)

Firstly, local net precipitation (P-E) in the southern Norwegian Sea was larger for MIS3 compared to the LGM conditions (Fig. 5), which can be attributed to the smaller Laurentide ice sheet. Eisenman et al. (2009) demonstrated the mechanism using the same climate model: a reduced ice sheet size causes the stationary wind field to become more northward over the northern North Atlantic/Nordic Seas and increases transient eddy activity due to a northward migration of the jet stream. Both processes increase the northward transport of moisture in the region and hence the local net precipitation.

Secondly, the freshwater transport out of the Arctic Ocean and into the southern Norwegian Sea via the East Greenland Current and the Nordic Seas' cyclonic gyre was much larger in MIS3 compared to in the LGM. This can be attributed to a freshening of the Arctic and subarctic seas due to the larger transport of water vapor from low to high latitudes under MIS3 conditions (Fig. 6). This strengthening of the hydrologic cycle can largely be explained by a significant thermodynamic contribution (cf. Held and Soden, 2006) in the relatively warmer MIS3 climate (Fig. 7), which, in turn, was mainly attributable to higher atmospheric greenhouse gas concentrations. An additional effect of the strengthened hydrologic cycle was enhanced net evaporation in the subtropical North Atlantic, leading to saltier upper-ocean waters in MIS3, which were partly advected northward into the Nordic Seas, where they were locally capped by the fresher surface waters, notably in the southern Norwegian Sea. This salt inflow from the south maintained a strong AMOC in the MIS3 baseline state.

Thirdly, in the colder LGM climate, a larger portion of the Arctic sea ice could make it further south into the mid-latitude North Atlantic, where it would melt south of Newfoundland (Fig. 8). By contrast, much more sea ice melted in the Nordic Seas under MIS3 conditions, leading to additional freshening of the Nordic Seas' surface waters.

4. Discussion

Numerous mechanisms have been proposed to explain D-O-type millennial-scale variability, including forced and spontaneous (unforced) changes in the AMOC (see Li and Born, 2019 and the references therein). Most hypotheses about the physical mechanisms have been based on studies with highly simplified or low-

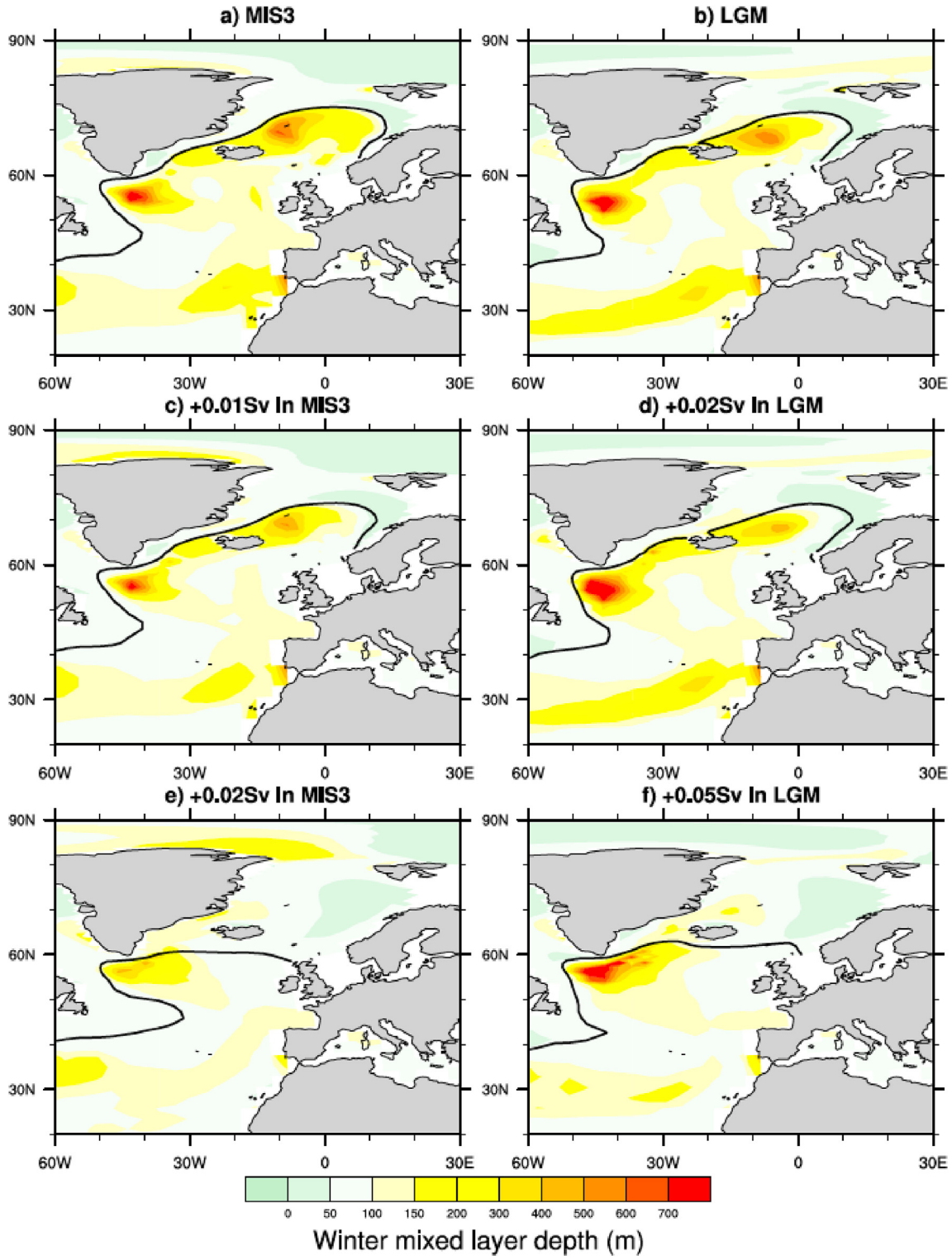

Fig. 3. Winter (December–February) mean mixed layer depths (m), indicating convective sites, along with winter sea ice margins (black contours; 50% mean sea ice concentration) for the unperturbed baseline states (a, b), for freshwater-perturbed states just left of the AMOC stability thresholds (c, d), and for freshwater-perturbed states just right of the thresholds (e, f), i.e. stadial states with weak AMOC. The left column is for MIS3 conditions, while the right column is for LGM conditions.

order models or with Earth-system models of intermediate complexity (see Timmermann et al., 2003 and the references therein). Some of the proposed mechanisms could only recently be reproduced in comprehensive AOGCMs. Klockmann et al. (2018) found unforced millennial-scale AMOC oscillations in AOGCM experiments with atmospheric CO_2 concentrations between 190 and 217 ppm but only with a modern ice sheet configuration. Brown and Galbraith (2016) found similar oscillations between a weak and a strong AMOC state, triggered by internal climate variability, in AOGCM simulations under a particular set of boundary

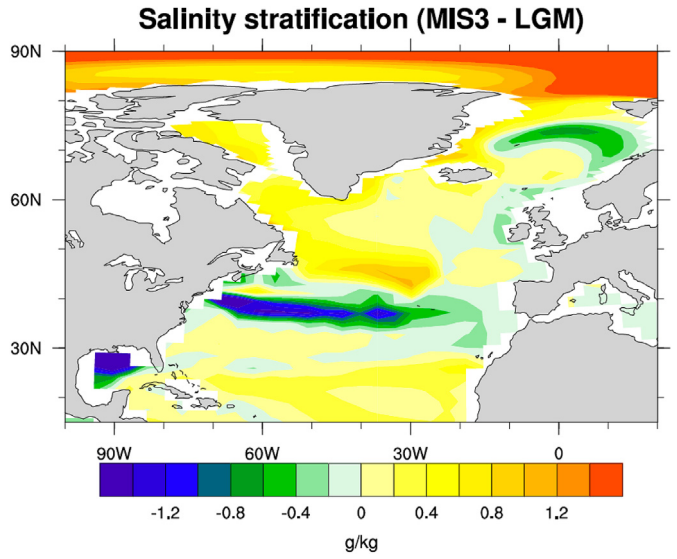

Fig. 4. Difference in salinity stratification between the MIS3 and LGM baseline states (MIS3−LGM). Salinity stratification is defined as the difference in salinity between 500 m and the sea surface (annual means), i.e. positive (negative) values indicate stronger (weaker) stratification in MIS3 compared to LGM.

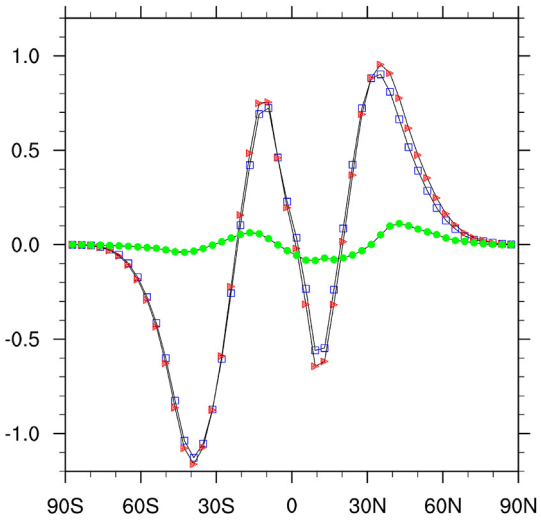

Fig. 6. Total northward atmospheric water vapor transport (Sv; annual mean) for the MIS3 (red triangles) and LGM (blue squares) baseline states as well as the difference (MIS3−LGM; green dots) as a function of latitude. (For interpretation of the references to colour in this figure legend, the reader is referred to the Web version of this article.)

conditions, characterized again by low CO_2 (180 ppm) and modern ice sheets. Although the models of Klockmann et al. (2018) and Brown and Galbraith (2016) do not simulate oscillations under true MIS3 conditions, these results suggest that "sweet spots" may exist where the climate system is prone to unforced millennial-scale oscillations (see also Galbraith and de Lavergne, 2019). However, the boundary conditions for which such sweet spots occur are likely model dependent. For instance, Kleppin et al. (2015) and Klus et al. (2019) found spontaneous AMOC state transitions under pre-industrial and late Holocene boundary conditions, respectively. Peltier and Vettoretti (2014) found self-sustained nonlinear oscillations of the coupled atmosphere−ocean−sea ice system in AOGCM simulations under full glacial (LGM) conditions (see also Vettoretti and Peltier, 2018). These studies doubtlessly provide important insights into potential mechanisms of millennial-scale climate variability; however, they obviously do not explain the preferred occurrence of D-O variability during MIS3 and its absence under full glacial conditions.

Two recent studies have addressed this issue. Like our present study, these AOGCM studies relied on forced AMOC transitions rather than unforced atmosphere-ocean-sea ice oscillations. Assuming that millennial-scale variability is caused by anomalous freshwater fluxes, Kawamura et al. (2017) found a much stronger climate response to freshwater anomalies under intermediate glacial conditions than under full glacial (LGM) and interglacial (pre-industrial) conditions, offering a possible explanation for the prevalent occurrence of D-O variability under intermediate conditions. The authors found that the unperturbed full glacial AMOC was exceptionally weak (only about 6 Sv) and hence could hardly be further weakened, such that freshwater hosing did not substantially impact the large-scale climate. However, such a weak AMOC under LGM conditions is supported by neither proxy data (Fig. 1; Lippold et al., 2012) nor dynamical reconstructions (Kurahashi-Nakamura, 2017), challenging the conclusions by Kawamura et al. (2017). In another study, Zhang et al. (2017) found a regime of AMOC bi-stability for intermediate ice sheet and CO_2 conditions, roughly corresponding to MIS3 conditions, whereas the full glacial and interglacial climates were mono-stable in their

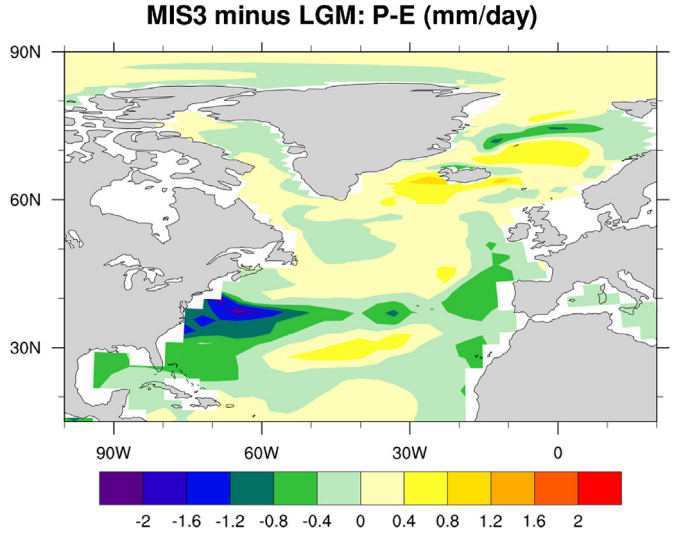

Fig. 5. Net precipitation (precipitation minus evaporation; mm/day) difference between the MIS3 and LGM baseline states (MIS3−LGM; annual mean).

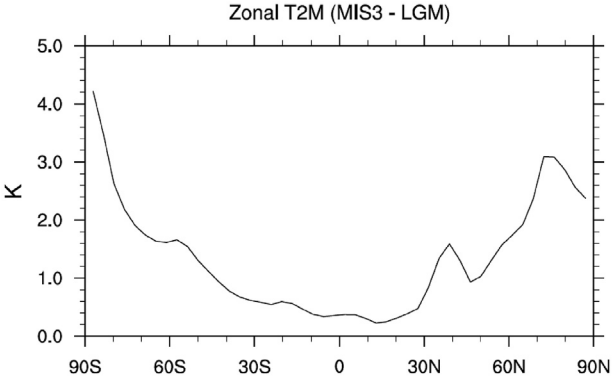

Fig. 7. Zonal mean 2-m air temperature (K) difference between MIS3 and LGM baseline states (MIS3−LGM; annual mean) as a function of latitude.

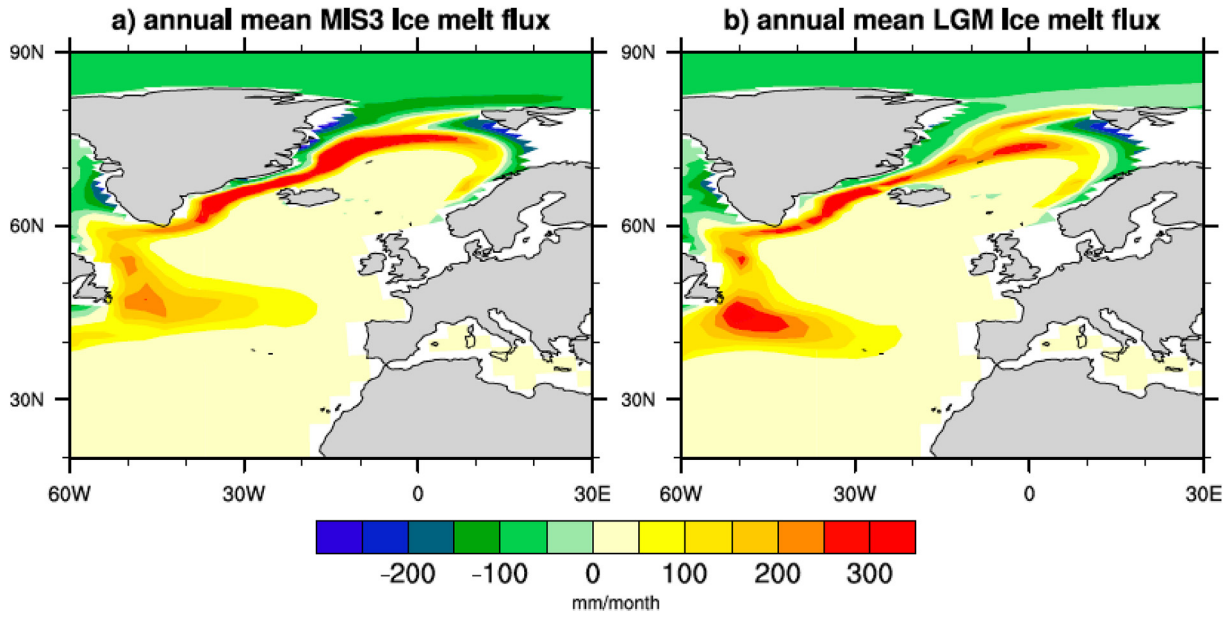

Fig. 8. Sea ice melt flux (mm/month) for the MIS3 (a) and LGM (b) baseline states (annual means). Negative values indicate net freezing.

AOGCM. In the bi-stable intermediate glacial regime, abrupt transitions from the strong to the weak AMOC state and vice versa could be triggered by not only freshwater perturbations but also gradual changes in atmospheric CO_2 or ice sheet height (Zhang et al. 2014a, 2017). However, the weaknesses of this model include the almost lacking climate response in the Nordic Seas and the small interstadial-stadial temperature difference in Greenland of less than 3 °C (Zhang et al. 2014a, 2017). This weak response in the D-O "centers of action" can be attributed to sea ice completely covering the Nordic Seas even in the strong (interstadial) AMOC mode (Fig. 4 in Zhang et al., 2014a), which contrasts with sea ice reconstructions revealing ice-free conditions in the Norwegian Sea during MIS3 interstadials (Hoff et al., 2016). This mismatch may indicate that the climate simulated in that study is too cold in high northern latitudes despite the intermediate boundary conditions. By contrast, the MIS3 interstadial (strong AMOC) and stadial (weak AMOC) states simulated in our CCSM3 experiments better match the reconstructed sea ice covers and temperatures in the polar and subpolar northern regions (Fig. 3; Zhang et al., 2014b; Zhang et al., 2015). Sea ice in the Nordic Seas not only plays a key role in our convective instability mechanism and the nonlinearity in the AMOC stability diagram (Fig. 2) but is also crucial for the temporal behavior and the magnitude of Greenland temperature changes (Zhang et al., 2014b; Li et al., 2010).

In our experiments, transitions from one state to the other require continuous freshwater flux anomalies in the Nordic Seas. Such freshwater anomalies can have manifold origins, but continental ice sheets have often been suggested to be responsible for storing and releasing this freshwater (e.g. Birchfield et al., 1994). There is indeed evidence from ice-rafted debris for increased iceberg and hence meltwater fluxes into the Nordic Seas during D-O stadials (Elliot et al., 2002; Dokken and Jansen, 1999; Voelker et al., 1998), likely related to internal coastal ice sheet dynamics in east Greenland (van Kreveld et al., 2000) and Fennoscandia (Elliot et al., 2002). Previous studies have already shown that freshwater-forced transient model simulations can effectively reproduce the spatiotemporal behavior of D-O millennial-scale climate variability (Ganopolski and Rahmstorf, 2001; Menviel et al., 2014). In particular, using an oxygen isotope-enabled climate model to simulate freshwater-driven D-O events, Bagniewski et al. (2017) have shown good agreement between simulated results and sediment records, thus providing further evidence for a link between stadial-interstadial climate variability, AMOC changes and continental ice-sheet instabilities. According to our CCSM3 results, minor perturbations in the freshwater forcing of the ocean could have triggered D-O climate transitions during the intermediate glacial climate of MIS3, when the baseline climate was close to the AMOC stability threshold and hence remarkably unstable, but not during the full glacial climate of the LGM, when the AMOC stability threshold was shifted to the right. However, larger meltwater fluxes (0.05 Sv or greater) would have substantially weakened the AMOC in both climates, which explains the occurrence of Heinrich Stadials under both full glacial (Heinrich Stadial 1) and intermediate glacial (in particular, Heinrich Stadial 4) conditions. Due to the absence of European ice sheets, which could have provided the necessary calving and meltwater, this concept also implies the absence of D-O-type variability during interglacials.

Due to the proximity of the MIS3 baseline climate state to the AMOC stability threshold, the unperturbed MIS3 climate cannot unequivocally be assigned to a stadial (Merkel et al., 2010) or interstadial (Van Meerbeeck et al., 2009; Gong et al., 2013; Guo et al., 2019) state, as done in previous MIS3 model studies. By contrast, the unperturbed LGM is associated with an "interstadial-type" (i.e. a relatively strong) AMOC state with a relatively large distance from the stability threshold. Proxy records underpin the concept of an interstadial-type AMOC during the LGM (Fig. 1).

We finally note that CCSM3's ocean component does not include a tidal mixing parameterization. Tidal mixing would possibly have an effect on the glacial AMOC and its stability. During the LGM, tidal dissipation was strongly increased due to the lower sea level (Schmittner et al., 2015; Wilmes et al., 2019). Larger diapycnal diffusivities in the Atlantic Ocean would have strengthened the AMOC and possibly increased its stability (Schmittner and Weaver, 2001; Prange et al., 2003). As such, including the effects of tidal mixing could further stabilize the AMOC of the LGM. However, compared to MIS3, this effect would be relatively small because major shelf sea areas were lost for tidal energy dissipation during

both the LGM and MIS3.

5. Conclusions

Millennial-scale variability associated with D-O events is most pronounced under intermediate glacial climate conditions like MIS3 and tied to variations in the AMOC. By contrast, full glacial (e.g. LGM) conditions are unfavorable for D-O-type climate variability. Based on experiments with CCSM3 – a coupled climate model that realistically simulates interstadial/stadial changes in Greenland's temperature and the Nordic Seas' ice cover – we find that the AMOC is less sensitive to freshwater perturbations under LGM conditions than under MIS3 conditions. The different stability properties can mainly be attributed to differences in the atmospheric hydrologic cycle and sea ice transports. Higher AMOC stability during the LGM compared to during the MIS3 provides a physically plausible explanation for why millennial-scale variability was suppressed under full glacial conditions and suggests that under intermediate glacial conditions, minor perturbations in the ocean surface freshwater forcing, e.g. related to ice sheet processes, could have triggered D-O-type climate shifts associated with a threshold in the atmosphere-ocean-sea ice system, whereas similar perturbations were ineffective during full glacials.

Statement

Xiao Zhang performed model simulation in this study. Xiao Zhang and Matthias Prange both contributed to modeling results analysis and manuscript writing. All authors reviewed and approved the manuscript prior to submission.

Declaration of competing interest

The authors declare that they have no known competing financial interests or personal relationships that could have appeared to influence the work reported in this paper.

Acknowledgments

This work was supported by the PalMod project funded by the German Federal Ministry of Education and Science (BMBF), the DFG Research Center/Cluster of Excellence "The Ocean in the Earth System" at the University of Bremen (MARUM), and the Young Scientists Fund from the National Natural Science Foundation of China (NSFC, project number 41605044). The model experiments were run on the supercomputer at the Norddeutscher Verbund für Hoch-und Höchstleistungsrechnen (HLRN).

References

Ahn, J., Brook, E.J., 2007. Atmospheric CO2 and climate from 65 to 39 ka BP. Geophys. Res. Lett. 34, L10703. https://doi.org/10.1029/2007GL029551.
Bagniewski, W., Meissner, K.J., Menviel, L., 2017. Exploring the oxygen isotope fingerprint of Dansgaard-Oeschger variability and Heinrich events. Quat. Sci. Rev. 159, 1–14.
Bereiter, B., et al., 2012. Mode change of millennial CO2 variability during the last glacial cycle associated with a bipolar marine carbon seesaw. Proc. Natl. Acad. Sci. U.S.A. 109, 9755–9760.
Birchfield, G.E., Wang, H., Rich, J.J., 1994. Century/millennium internal climate oscillations in an ocean-atmosphere-continental ice sheet model. J. Geophys. Res. 99, 12459–12470.
Braconnot, P., et al., 2007. Results of PMIP2 coupled simulations of the mid-Holocene and Last Glacial maximum, part 1: experiments and large-scale features. Clim. Past 3, 261–277.
Brown, N., Galbraith, E.D., 2016. Hosed vs. unhosed: interruptions of the Atlantic Meridional Overturning Circulation in a global coupled model, with and without freshwater forcing. Clim. Past 12, 1663–1679. https://doi.org/10.5194/cp-12-1663-2016.
Collins, D.W., et al., 2006. The community climate system model version 3 (CCSM3). J. Clim. 19, 2122–2143.
Dokken, T.M., Jansen, E., 1999. Rapid changes in the mechanism of ocean convection during the last glacial period. Nature 401, 458–461.
Eisenman, I., Bitz, C.M., Tziperman, E., 2009. Rain driven by receding ice sheets as a Cause of past climate change. Paleoceanography 24, PA4209. https://doi.org/10.1029/2009PA001778.
Elliot, M.L., Labeyrie, L., Duplessy, J.C., 2002. Changes in North Atlantic deep-water formation associated with the Dansgaard-Oeschger temperature oscillations (60–10ka). Quat. Sci. Rev. 21 (10), 1153–1165.
EPICA Community Members, 2006. One-to-one coupling of glacial climate variability in Greenland and Antarctica. Nature 444, 195–198.
Flückiger, J., Blunier, T., Stauffer, B., Chappellaz, J., Spahni, R., Kawamura, K., Schwander, J., Stocker, T.F., Dahl-Jensen, D., 2004. N2O and CH4 variations during the last glacial epoch: insight into global processes. Global Biogeochem. Cycles 18, GB1020. https://doi.org/10.1029/2003GB002122.
Galbraith, E., de Lavergne, C., 2019. Response of a comprehensive climate model to a broad range of external forcings: relevance for deep ocean ventilation and the development of late Cenozoic ice ages. Clim. Dynam. https://doi.org/10.1007/s00382-018-4157-8.
Ganopolski, A., Rahmstorf, S., 2001. Rapid changes of glacial climate simulated in a coupled climate model. Nature 409, 153–158.
Gong, X., Knorr, G., Lohmann, G., 2013. Dependence of abrupt Atlantic meridional ocean circulation changes on climate background states. Geophys. Res. Lett. 40, 3691–3704. https://doi.org/10.1002/grl.50701.
Grootes, P.M., Stuiver, M., 1997. Oxygen 18/16 variability in Greenland snow and ice with 10-3- to 105-year time resolution. J. Geophys. Res. 102 (C12), 26455–26470.
Guo, et al., 2019. Equilibrium simulations of marine isotope stage 3 climate. Clim. Past 15, 1133–1151.
Held, I., Soden, B., 2006. Robust responses of the hydrological cycle to global warming. J. Clim. 19, 5686–5699.
Henry, et al., 2016. North Atlantic ocean circulation and abrupt climate change during the last glaciation. Science 353, 470–474.
Hoff, et al., 2016. Sea ice and millennial-scale climate variability in the Nordic seas 90 ka to present. Nat. Commun. https://doi.org/10.1038/ncomms12247.
Huber, C., et al., 2006. Isotope calibrated Greenland temperature record over Marine Isotope Stage 3 and its relation to CH4. Earth Planet Sci. Lett. 243, 504–519.
Kawamura, K., et al., 2017. State dependence of climatic instability over the past 720,000 years from Antarctic ice cores and climate modeling. Sci. Adv. 3, e1600446.
Kindler, P., et al., 2014. Temperature reconstruction from 10 to 120 kyr b2k from the NGRIP ice core. Clim. Past 10, 887–902.
Kleppin, H., Jochum, M., Otto-Bliesner, B., Shields, C.A., Yeager, S., 2015. Stochastic atmospheric forcing as a cause of Greenland climate transitions. J. Clim. 28, 7741–7763.
Klockmann, M., Mikolajewicz, U., Marotzke, J., 2018. Two AMOC states in response to decreasing greenhouse gas concentrations in the coupled climate model MPI-ESM. J. Clim. 31 (19), 7969–7984.
Klus, A., Prange, M., Varma, V., Schulz, M., 2019. Spatial analysis of early-warning signals for a North Atlantic climate transition in a coupled GCM. Clim. Dynam. 53, 97–113. https://doi.org/10.1007/s00382-018-4567-7.
Kurahashi-Nakamura, Takasumi, et al., 2017. Dynamical reconstruction of the global ocean state during the Last Glacial Maximum. Paleoceanography 32.
Landais, A., et al., 2004. A continuous record of temperature evolution over a sequence of Dansgaard–Oeschger events during Marine Isotopic Stage 4 (76 to 62 kyr BP). Geophys. Res. Lett. 31, L22211. https://doi.org/10.21029/22004GL021193.
Li, C., Born, A., 2019. Coupled atmosphere-ice-ocean dynamics in Dansgaard-Oeschger events. Quat. Sci. Rev. 203 (5020), 1–20.
Li, C., Battisti, D.S., Bitz, C.M., 2010. Can North Atlantic sea ice anomalies account for Dansgaard–Oeschger climate signals? J. Clim. 23, 5457–5475.
Lippold, J., et al., 2009. Does sedimentary 231 Pa/230Th from the Bermuda Rise monitor past atlantic meridional overturning circulation? Geophys. Res. Lett. 36, L12601. https://doi.org/10.1029/2009GL038068.
Lippold, J., et al., 2012. Strength and geometry of the glacial atlantic meridional overturning circulation. Nat. Geosci. 5, 813–816. https://doi.org/10.1038/ngeo1608.
McManus, J.F., et al., 2004. Collapse and rapid resumption of Atlantic meridional circulation linked to deglacial climate changes. Nature 428, 834–837.
Menviel, L., Timmermann, A., Friedrich, T., England, M.H., 2014. Hindcasting the continuum of Dansgaard–Oeschger variability: mechanisms, patterns and timing. Clim. Past 10, 63–77. https://doi.org/10.5194/cp-10-63-2014, 2014.
Merkel, U., Prange, M., Schulz, M., 2010. ENSO variability and teleconnections during glacial climates. Quat. Sci. Rev. 29, 86–100.
Mohtadi, M., Prange, M., Oppo, Delia W., De Pol-Holz, R., Merkel, U., Zhang, X., Steinke, S., Lückge, A., 2014. North Atlantic forcing of tropical Indian Ocean climate. Nature 509, 76–80.
Oleson, K.W., et al., 2008. Improvements to the Community Land Model and their impact on the hydrological cycle. J. Geophys. Res. 113, G01021. https://doi.org/10.1029/2007JG000563.
Otto-Bliesner, B., Brady, E.C., Clauzet, G., Tomas, R., Levis, S., Kothavala, Z., 2006. Last glacial maximum and Holocene climate in CCSM3. J. Clim. 19, 2526–2544.
Peltier, W.R., 2004. Global glacial isostasy and the surface of the ice-age Earth: the ICE-5G (VM2) model and GRACE. Annu. Rev. Earth Planet Sci. 32, 111–149.
Peltier and Vettoretti, 2014. Dansgaard-Oeschger oscillations predicted in a

comprehensive model of glacial climate: a kicked salt oscillator in the Atlantic. Geophys. Res. Lett. 41 (20), 7306–7313, 2014GL061413.
Prange, M., Gerdes, R., 2006. The role of surface freshwater flux boundary conditions in Arctic Ocean modelling. Ocean Model. 13, 25–43.
Prange, M., Lohmann, G., Gerdes, R., 1997. Sensitivity of the thermohaline circulation for different climates - investigations with a simple atmosphere-ocean model. Palaeoclim 2, 71–99.
Prange, M., Romanova, V., Lohmann, G., 2002. The glacial thermohaline circulation: stable or unstable? Geophys. Res. Lett. 29 (21), 2028. https://doi.org/10.1029/2002GL015337.
Prange, M., Lohmann, G., Paul, A., 2003. Influence of vertical mixing on the thermohaline hysteresis: analyses of an OGCM. J. Phys. Oceanogr. 33 (8), 1707–1721.
Romanova, V., Prange, M., Lohmann, G., 2004. Stability of the glacial thermohaline circulation and its dependence on the background hydrological cycle. Clim. Dynam. 527–538.
Sarnthein, M., et al., 2001. Fundamental modes and abrupt changes in North Atlantic circulation and climate over the last 60 ky – concepts, reconstructions and numerical modeling. In: Schäfer, P., et al. (Eds.), The Northern North Atlantic: A Changing Environment. Springer-Verlag, New York, pp. 365–410.
Schmittner, A., Weaver, A.J., 2001. Dependence of multiple climate states on ocean mixing parameters. Geophys. Res. Lett. 28, 1027–1030.
Schmittner, A., Green, J.A.M., Wilmes, S.B., 2015. Glacial ocean overturning intensified by tidal mixing in a global circulation model. Geophys. Res. Lett. 42 (10), 4014–4022. https://doi.org/10.1002/2015GL063561.
Schulz, M., Berger, W.H., Sarnthein, M., Grootes, P.M., 1999. Amplitude variations of 1470-year climate oscillations during the last 100,000 years linked to fluctuations of continental ice mass. Geophys. Res. Lett. 26 (22), 3385–3388. https://doi.org/10.1029/1999GL006069.
Spahni, R., et al., 2005. Atmospheric methane and nitrous oxide of the late Pleistocene from Antarctic ice cores. Science 310, 1317–1321.
Timmermann, A., Gildor, H., Schulz, M., Tziperman, E., 2003. Coherent resonant millennial-scale climate oscillations triggered by massive meltwater pulses. J. Clim. 16, 2569–2585. https://doi.org/10.1175/1520-0442(2003)016<2569:CRMCOT>2.0.CO;2.
van Kreveld, S.A., Sarnthein, M., Erlenkeuser, H., Grootes, P., Jung, S., Nadeau, M.J., Pflaumann, U., Voelker, A., 2000. Potential links between surging ice sheets, circulation changes, and the Dansgaard-Oeschger cycles in the Irminger Sea, 60–18 kyr. Paleoceanography 15 (4). https://doi.org/10.1029/1999PA000464.
Van Meerbeeck, C.J., Renssen, H., Roche, D.M., 2009. How did marine isotope stage 3 and LastGlacial maximum climates differ?—perspectives from equilibrium simulations. Clim. Past 5, 33–51.
Vettoretti, G., Peltier, W.R., 2018. Fast physics and slow physics in the nonlinear Dansgaard-Oeschger relaxation oscillation. J. Clim. https://doi.org/10.1175/JCLI-D-17-0559.1.
Voelker, A.H.L., 2002. Global distribution of centennial-scale records for marine istope state (MIS) 3: a database. workshop participants Quat. Sci. Rev. 21, 1185–1214.
Voelker, A.H.L., Samthein, M., Grootes, P.M., Erlenkeuser, H., Laj, C., Mazaud, A., Nadeau, M.-J., Schleicher, M., 1998. Correlation of marine C14 ages from the Nordic Seas with the GISP2 isotope record: implications for radiocarbon calibration beyond 25 ka BP. Radiocarbon 40, 517–534.
Wilmes, S.-B., Schmittner, A., Green, J.A.M., 2019. Glacial ice sheet extent effects on modeled tidal mixing and the global overturning circulation. Paleoceanogr. Paleoclim. https://doi.org/10.1029/2019PA003644.
Yeager, S.G., Shields, C.A., Large, W.G., Hack, J.J., 2006. The low-resolution CCSM3. J. Clim. 19, 2545–2566.
Zhang, X., Lohmann, G., Knorr, G., Purcell, C., 2014a. Abrupt glacial climate shifts controlled by ice sheet changes. Nature 512, 290–294. https://doi.org/10.1038/nature13592.
Zhang, X., Prange, M., Merkel, U., Schulz, M., 2014b. Instability of the atlantic overturning circulation during marine isotope stage 3. Geophys. Res. Lett. 41 https://doi.org/10.1002/2014GL060321.
Zhang, X., Prange, M., Merkel, U., Schulz, M., 2015. Spatial fingerprint and magnitude of changes in the Atlantic meridional overturning circulation during Marine Isotope Stage 3. Geophys. Res. Lett. 42 https://doi.org/10.1002/2014GL063003.
Zhang, X., Knorr, G., Lohmann, G., Barker, S., 2017. Abrupt North Atlantic circulation changes in response to gradual CO2 forcing in a glacial climate state. Nat. Geosci. 10, 518–523.